

NASA-TM-88186 19860004735

---

# Focal Plane Optics in Far-Infrared and Submillimeter Astronomy

---

Roger H. Hildebrand

---

LIBRARY COPY

NOV 12 1985

October 1985

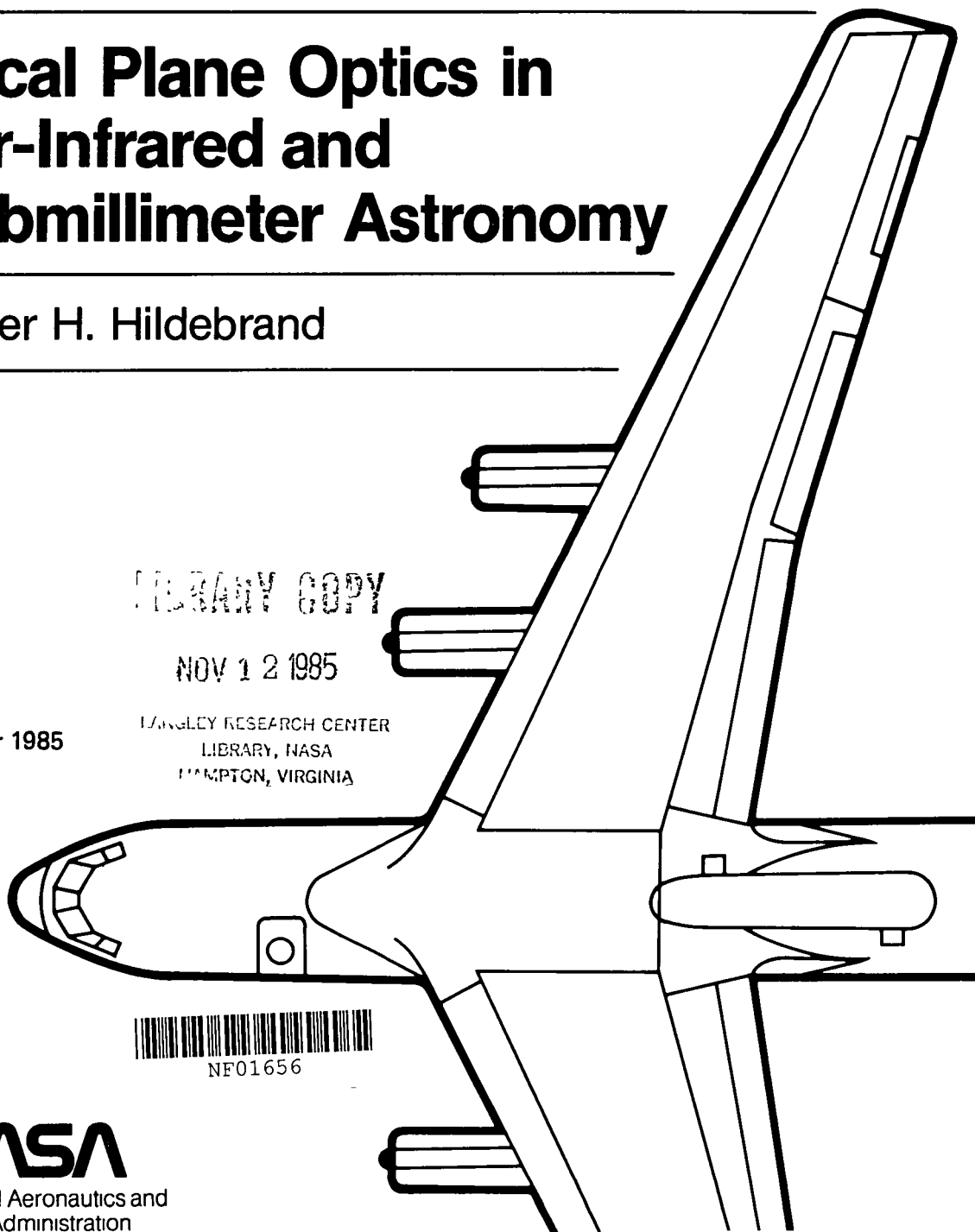
LANGLEY RESEARCH CENTER  
LIBRARY, NASA  
HAMPTON, VIRGINIA



NF01656

**NASA**

National Aeronautics and  
Space Administration



---

# Focal Plane Optics in Far-Infrared and Submillimeter Astronomy

---

Roger H. Hildebrand, Enrico Fermi Institute, University of Chicago, Chicago, Illinois

October 1985



National Aeronautics and  
Space Administration

**Ames Research Center**  
Moffett Field, California 94035

*N86-14204 #*

# Focal plane optics in far-infrared and submillimeter astronomy

Roger H. Hildebrand

Enrico Fermi Institute, Department of Physics, and

Department of Astronomy and Astrophysics

The University of Chicago, 5640 South Ellis Avenue

Chicago, Illinois 60637

## CONTENTS

1. Introduction
2. General characteristics of far-IR field optics
3. Winston concentrators
4. Cavity design
5. Optical properties of bolometers
6. Re-imaging optics
7. Reflector fabrication
8. Lens materials
9. Spectral filters
10. Polarimeters
11. Acknowledgements
12. References

## Abstract

The construction of airborne observatories, high mountain-top observatories, and space observatories designed especially for infrared and submillimeter astronomy has opened fields of research requiring new optical techniques. A typical far-IR photometric study involves measurement of a continuum spectrum

in several passbands between  $\sim 30\mu\text{m}$  and  $1000\mu\text{m}$  and diffraction-limited mapping of the source. At these wavelengths, diffraction effects strongly influence the design of the field optics systems which couple the incoming flux to the radiation sensors (cold bolometers). The Airy diffraction disk for a typical telescope at submillimeter wavelengths ( $\sim 100\mu\text{m} - 1000\mu\text{m}$ ) is many millimeters in diameter; the size of the field stop must be comparable. The dilute radiation at the stop is fed through a Winston nonimaging concentrator to a small cavity containing the bolometer.

The purpose of this paper is to review the principles and techniques of infrared field optics systems, including spectral filters, concentrators, cavities, and bolometers (as optical elements), with emphasis on photometric systems for wavelengths longer than  $60\mu\text{m}$ .

Keywords: nonimaging optics; field optics, infrared; submillimeter; astronomy; photometry

## 1. INTRODUCTION

The prospects for astronomy at wavelengths beyond a few microns were greatly improved when, in 1961, Frank Low constructed a cold germanium bolometer with a sensitivity approaching the limits set by thermodynamics.<sup>1</sup> For the first time one could seriously consider far-infrared observations of cold interstellar clouds, distant galaxies, and other faint celestial objects.

To realize such observations, the cold bolometer had to be put at the focal plane of a telescope on a high mountain top or on some other platform above most of the earth's atmospheric water vapor with provision for subtracting background radiation from the sky and for selecting the desired infrared wavelengths.

The solutions to these and associated problems were well advanced by the late 1960's. In their paper of 1974, Low and Rieke<sup>2</sup> gave a brief historical review of infrared instrumentation and a comprehensive presentation of the state of the art at that time. It is still an excellent reference for anyone entering the field. The emphasis of that review is on photometry at wavelengths less than  $30\mu\text{m}$ .

I shall present here a narrower review confined to field optics with emphasis on photometry at wavelengths greater than  $60\mu\text{m}$ . In either range of wavelengths a field optics system is essential to restrict the view of the detector to the telescope mirror: an unrestricted view would expose the detector to a flood of thermal radiation from surrounding ambient-temperature objects. Other functions of the field optics vary according to the wavelength. At ten or twenty microns the image of a point source is smaller than the smallest practical size of a detector (i.e., smaller than a few tenths of a millimeter) and one relies on the field optics to spread the energy from any point within the field stop over the entire detector to overcome any nonuniform response over the detector area. At 100 or 200 microns the diffraction image of a point source is much larger than the size of the detector and one relies on the field optics to concentrate the radiation by a large factor (typically hundreds or thousands) and couple it efficiently to a radiation sensor. Since I am a colleague of Roland Winston's I could hardly escape noticing that that is a job for nonimaging concentrators.<sup>3,4</sup> In 1974, I enlisted the aid of Winston, Harper, and Stiening and after more trouble than we expected, we produced an efficient system, which we call a heat trap,<sup>5</sup> for diffraction limited applications in the far-infrared and submillimeter (SMM) regions.

I shall review what is now known about such systems, and how to handle some of the practical engineering problems that are not mentioned in previous literature.

## 2. GENERAL CHARACTERISTICS OF FAR-IR FIELD OPTICS

A field optics system for far-IR photometry usually includes a spectral filter, a field stop, a concentrator (a lens, mirror, or Winston concentrator<sup>3,4</sup>), a cavity fed by the concentrator, and a bolometer suspended in the cavity. Such a system is shown schematically in Figure 1. The radius of the field stop (stop sometimes provided by reflector aperture) is set to give the desired beam radius (i.e., the radius of the antenna pattern, FWHM) or to give the desired trade-off between angular resolution and throughput (cf. Figure 2). The reflector and lens together compose the concentrator (no lens is used for a compound parabolic concentrator). The concentrator, cavity, and bolometer together compose a heat trap. The bolometer is suspended in the cavity from the leads which supply the bias current. The leads enter the cavity through small slots.

The dimensions of the system depend on the wavelength band passed by the filter and on the focal ratio,  $f$ , of the telescope. Where angular resolution and throughput are both important, the radius of the field stop is made equal to or somewhat less than the radius,  $\delta = 1.22\lambda f$ , of the Airy disk. The dependence of angular resolution on aperture size, as computed from the convolution of the aperture with the diffraction image of a point source, is shown in Fig. 2a. In computing the dependence of throughput on aperture size one must take into account the contribution of the field stop itself to diffraction effects in the concentrator. A curve showing the solution to that problem for point sources is given in Fig. 2b.<sup>6</sup>

The acceptance angle of the field optics,  $\theta_1$ , is chosen close to the angle,  $\arcsin(1/2f)$ , of the peripheral rays reaching the field stop from the telescope mirror (usually the secondary mirror). A slightly larger value insures acceptance of all rays from the mirror; a slightly smaller value insures exclusion of stray rays. It is not possible, without loss of performance, to adapt a Winston concentrator of one acceptance angle,  $\theta_1$ , to a telescope requiring a different acceptance angle,  $\theta_1'$ , simply by using a lens ahead of the focal plane to redirect the peripheral rays from  $\theta_1'$  to  $\theta_1$ . Consider first the case with no lens (Figure 3a). Since the field stop is very small compared to the dimensions of the telescope, the range of angles, 0 to  $\theta_1'$ , of rays reaching the focal plane is very nearly the same at every point within the field stop. When a lens is inserted (Figure 3b), the range of angles reaching the center of the field becomes 0 to  $\theta_1$ ; the range at other points depends on the distance from the center. Hence the throughput of the system is reduced and stray rays are accepted. It is possible and often desirable to incorporate a lens in an efficient field optics system, but only if the figure of the reflecting surface of the Winston concentrator is appropriately modified or the telescope mirror is re-imaged onto the field stop. (See later sections.)

The relationship between the diameters,  $d_1$  and  $d_2$ , of the entrance and exit apertures of an ideal concentrator is governed by the general condition that the integral,  $\int \vec{A} \cdot d\vec{\Omega}$ , of the projected area over the solid angle is conserved when radiation passes through an optical system without losses. If an entrance aperture of area  $A_1 = \pi(d_1/2)^2$  accepts radiation from angles zero to  $\theta_1$ , and if the area,  $A_2 = \pi(d_2/2)^2$ , of the exit aperture is made as small as possible then one must have  $\theta_2 = \pi/2$  and

$$d_2 = d_1 \sin \theta_1 = d_1/(2f). \quad (1)$$

Because of diffraction effects within the concentrator, the system cannot be entirely free of losses, but for  $d_1 = 2\delta = 2.44\lambda f$ ,  $d_2 = 1.22\lambda$  the diffraction loss

remains negligible. The loss is  $\sim 20\%$  at  $d_1 = 1.7\lambda f$ ,  $d_2 = 0.6\lambda$  and increases rapidly as the dimensions are further reduced.

The "diameter" (i.e., the smallest transverse dimension) of the radiation sensor is made somewhat larger than the larger of  $\lambda$  or  $d_2$ . If that is greater than the size of a sensor giving the best electrical noise equivalent power<sup>2</sup> (i.e., greater than a few tenths of a millimeter), then a composite structure is used to extend the collecting area without enlarging the sensor itself<sup>7</sup> (see section on bolometers).

The cavity is designed to contain the strongly divergent ( $2\pi$  ster. rad.) radiation emerging from the collector and to optimize its absorption by the radiation sensor. The bolometer, and hence the cavity and light collector, are operated at low temperatures (usually  $< 2$  K) in order to reduce the detector noise. The filter, field stop, and lens (when used) are operated at low enough temperatures (usually  $\leq 77$  K) so that they do not become significant sources of thermal radiation. To reduce exposure to room temperature radiation these components are protected by cold baffles.

### 3. WINSTON CONCENTRATORS

The principles of ideal concentrators have been reviewed for both geometrical<sup>3,4</sup> and diffraction limited<sup>5,6</sup> optics. For wavelengths  $\lambda \ll d_2$  the ideal concentrator achieves very nearly the maximum concentration of radiation,  $(d_1/d_2)^2 = (1/\sin \theta_1)^2$ , allowed by phase space conservation (equation (1)). A small loss of skew rays drops the concentration slightly below this value in all but the lens/trumpet design, the only truly ideal design (see below). As discussed in the last section, diffraction effects cause an additional loss when  $d_2 \lesssim \lambda$ .



The simplest design, the compound parabolic concentrator<sup>3,5</sup> (CPC), is generally preferred for use with small apertures and large acceptance angles (low  $f$ ). As  $d_1$  and  $f$  increase, the length of the collector,

$$L = d_1(2f + 1)(4f^2 - 1)^{1/2}/(4f), \quad (2)$$

becomes inconveniently large. For  $f \gg 1$  this expression becomes

$$L \approx d_1 f. \quad (3)$$

A CPC designed for 1 mm observations at  $f/35$ , the focal ratio used at some large IR telescopes, would have a length of more than 2-1/2 meters (for  $d_1 > 2\lambda f$ ), which is much too long to be contained in any cryostat now used in submillimeter photometry.

A much more compact design is achieved by incorporating a lens as a component of the light collector.<sup>8</sup> In this case the reflecting surface becomes a compound hyperbola. The lens/reflector system is called a compound hyperbolic concentrator (CHC) or, in early references, a lens-mirror CPC. To good approximation, the length of a CHC with a lens of focal ratio  $f_L$  is given by

$$L = d_1 f f_L / (f + f_L) \quad (4)$$

and is thus shorter than the CPC by approximately the factor  $f_L / (f + f_L)$ . For  $f = 35$ ,  $f_L = 2.1$  (the values for a millimeter photometer for the NASA/University of Hawaii Infrared Telescope Facility<sup>9</sup>), this factor is 0.057, and the length is reduced to 152 mm for  $d_1 = 2.2\lambda f$ ,  $\lambda = 1$  mm.

The aberrations of spherical lenses produce negligible effects in these collectors for  $f_L \gtrsim 2$ . Faster lenses can be used without loss if the system continues to satisfy the following conditions: (1) no caustic is formed between the lens and the reflecting surface, (2) rays entering at the extreme angle,  $\theta_1$ , are focused at the edge of the exit aperture, and (3)  $\int n ds = \text{constant}$ , where  $n$  is the index of refraction at the path element  $ds$  and the integral is taken along

the light path of rays at the extreme angle from the incident wavefront,  $w$ , to the focal point.

A third design, the lens/trumpet concentrator (LTC), described by Winston and Welford,<sup>10</sup> has not yet been applied to infrared photometry but may prove valuable because of its ideal beam pattern. The profile follows the configuration of electrostatic field lines from a charged conducting disk of diameter  $d_A$  originating from a circle of diameter  $d_2$ , where  $d_2$  is the diameter of the exit aperture and  $d_A$  is the diameter of the virtual image of the telescope mirror seen by the reflector (Figure 4). The length is approximately equal to that of the CHC. This design is unique in having no loss of skew rays. In the limit of geometrical optics the beam pattern is perfectly sharp. This ideal behavior is not precisely realized, even in the geometrical limit, when reflection losses are taken into account: the number of reflections becomes very large for rays near the acceptance angle. However, the number of reflections can be reduced with very little loss of concentration by slightly truncating the (nearly cylindrical) exit end of the concentrator. The average number of reflections vs  $\theta_1$  (and vs  $f$ ) is shown in Figure 5 for each type of concentrator. A technique for estimating the mean number of reflections in specular radiation passages has been presented by Rabl.<sup>11</sup> Reflectivities are generally very high in the far-IR and sub-millimeter regions.<sup>12</sup>

For all these designs, one can severely truncate the entrance end of the reflector with very little effect on the throughput or the angular response pattern. For the CPC, the loss is 10% when the length is reduced to 60% of the value given by equation (2).<sup>5</sup> For the CHC, the loss is  $\sim 10\%$  for  $l = 50\%$  of the value given by equation (4). No exact analysis or test of truncation has been made for the LTC, but the results should be similar to those for the CHC. For the CHC and LTC, truncation does not reduce the overall length: the lens must

remain at the position of the entrance aperture before the truncation. The reduction in length of the reflector can be important, however, in reducing the bulk of material to be held at the temperature of the bolometer. The gap between the lens and the reflector can be used for the field stop and filters.

All of the Winston concentrator designs are readily incorporated into close-packed arrays. A 36-element array has been designed by Harper for the Kuiper Airborne Observatory.

#### 4. CAVITY DESIGN

Radiation entering the cavity will eventually be absorbed by the bolometer or will escape through the apertures in the cavity walls. Losses at the highly reflecting surfaces of the cavity are generally negligible. The aperture admitting the radiation (the exit aperture of the concentrator) is constrained to a diameter  $d_2 \gtrsim \lambda$ . The apertures for the bolometer leads can be reduced to slots  $\sim 0.15 \text{ mm} \times 0.6 \text{ mm}$ ; i.e., to areas somewhat less than half of the area of the smallest bolometers now in common use (typically cubes  $\sim 0.25 \text{ mm}$  on a side.)

A large ratio of bolometer surface area to aperture area is not sufficient to assure that a large fraction of the energy will be absorbed. An element of the bolometer surface is effective only to the extent that it is exposed to the entering radiation. The design principle for the cavity is to maximize the solid angle in which each surface element views the sky or a reflection of the sky, and hence to minimize the solid angle in which each element views a reflection of the bolometer.<sup>4</sup> A spherical or hemispherical cavity is therefore an especially poor choice.<sup>5</sup> A cylindrical cavity of depth  $\approx$  diameter  $\approx 2d_2$  with the bolometer approximately centered is a much better choice.<sup>5</sup> The analysis of solar concentrator design by Welford and Winston<sup>4</sup> may serve as a guide for better

cavity designs, especially when the size, shape, and placement of bolometers can be controlled with better precision than is now achieved.

## 5. OPTICAL PROPERTIES OF BOLOMETERS

The thermal and electrical properties of bolometers have been discussed by Low and Rieke<sup>2</sup> and by Mather.<sup>13</sup> Doped silicon bolometers with ion implanted leads have been shown<sup>14,15</sup> to be ideal in having only the fundamental sources of electrical noise.<sup>13</sup> The absorptivity, however, is significantly less than ideal at submillimeter wavelengths for all known bolometer materials. (Hence, the importance of efficient cavity design.) Factors influencing the absorptivity include the wavelength and the ratio of wavelength to bolometer dimensions, as well as the intrinsic properties of the material.

In order to minimize the noise and heat capacity, the size of a bolometer is usually limited to a few tenths of a millimeter. In applications where values of  $\lambda$  and/or  $d_2$  necessitate larger sizes, one can increase the absorbing area without a corresponding increase in noise and heat capacity by bonding a dielectric substrate to the sensing element.<sup>7,16</sup> Typically, a diamond flake is bonded to the sensing element with epoxy. Since the substrate is itself a poor absorber, it is coated with a metal film of such a thickness that the reflectivity goes to zero; that is, so that

$$z_0/R = n - 1 \quad (4)$$

where  $z_0 = (\epsilon_0/\mu_0)^{1/2} = 377 \, \Omega$  = impedance of free space,  $R$  = surface resistance in ohms per square, and  $n$  = index of refraction of the substrate at wavelength  $\lambda$ . For the proper thickness, the Fresnel formulae<sup>7</sup> for the transmission and absorption reduce to  $t = 1/n$ ,  $a = (n - 1)/n$ . The values for diamond at 1 mm ( $n \approx 2.7$ ) are  $t = 0.37$ ,  $a = 0.63$ .

In principle, any metal can be used for the absorbing film, but since the heat capacity of the film may be large and strongly temperature dependent, one must consider both the required thicknesses and the specific heats of possible film metals at the intended operating temperatures. Bismuth<sup>7</sup> is a good choice for temperatures below  $\sim 0.3$  K (temperatures for  $^3\text{He}$  refrigeration). Gold is significantly better at  $T \geq 1$  K (temperatures for pumped  $^4\text{He}$  refrigeration).<sup>17</sup>

## 6. RE-IMAGING OPTICS

In the preceding discussion, we have described systems for maximum concentration of radiation. In some circumstances the performance can be improved by reducing the concentration below the limiting value  $(2f)^2$ . This is particularly true for  $\lambda < 100 \mu\text{m}$  where the limiting concentration may result in an exit aperture smaller than the smallest practical size for a bolometer. In a suitably designed system one may effect a trade between concentration and throughput, thereby reducing losses due to diffraction within the field optics. A corollary is improvement in the antenna pattern.

A reimaging system which realizes these improvements has been designed by Harper. A lens (or mirror) at the focal plane of the telescope reimages the telescope mirror at a second lens (or mirror). The second lens reimages the first (and again the telescope mirror) at the entrance plane of the light concentrator (Figure 6). Both lenses are cold so as not to introduce thermal radiation. The first is much larger than necessary to transmit the geometrical rays reaching the field stop at the entrance aperture of the light concentrator. The second lens is a pupil stop which is much larger than the field stop. The acceptance angle of the light collector is larger than necessary to contain the rays reaching the field stop but not so large as to require an unacceptably large detector. Accordingly, there is a negligible loss of throughput or degradation of the

antenna pattern due to diffraction by the field stop. No stray radiation reaches the field stop.

If instead of a single light concentrator, one uses an array in which each individual concentrator receives rays well removed from the edges of the first lens, and each accepts a wider range of angles than is covered by the pupil stop, then there will be negligible differences in performance between elements at the center and those at the edge of the array.

## 7 REFLECTOR FABRICATION

The first and most time-consuming step in producing a reflector is to make a mandrel whose outer surface follows the desired contour of the (inner) reflecting surface. The error in the radius,  $r$ , must be  $\ll \lambda$  and  $\ll d_2/2$  along the entire length. The error in the slope of the surface,  $dr/dz$ , must everywhere be  $\ll d_2/(2z)$ , where  $z$  is the distance from the exit aperture measured along the axis.<sup>5</sup> When the mandrel is to be re-used or pressed into copper, it is made of stainless steel; otherwise it is made of aluminum.

Two satisfactory techniques have been found to fabricate the reflector from the finished mandrel. One is to electroform nickel over the mandrel; the other is to press the mandrel into soft copper. In neither case is there difficulty in removing the reflector from the mandrel. The chief difficulty is in producing an exit aperture of the desired radius free of burrs or other imperfections. For this reason the mandrel does not end at the position of the exit aperture, but extends to a point. A clean aperture can be produced by grinding off the end of the reflector before removing the reflector from the mandrel, or by withdrawing the mandrel for later use and then grinding the end to the desired aperture and carefully hand-working the edge. No satisfactory replacement for the mandrel has yet been found for use during the grinding process.

## 8. LENS MATERIALS

Summaries of the optical constants of far-infrared materials have been given by several authors.<sup>18-20</sup> Two materials which have been used for far-IR and submillimeter lenses are TPX, a polyolefin resin marketed by Imperial Chemical Industries, and high density polyethylene. Both have very low dispersion over a wide wavelength range. TPX is convenient because of its transparency at optical wavelengths and because of the close match between the visible and far-IR indexes of refraction ( $n = 1.465$  optical;  $n = 1.45$  from  $\sim 30 \mu\text{m}$  to  $> 300 \mu\text{m}$ ). High density polyethylene ( $n = 1.52$  for  $\sim 60 \mu\text{m}$  to  $1000 \mu\text{m}$ ) is not optically transparent but it has lower absorption losses than TPX. The coefficients of absorption at  $200 \mu\text{m}$  are  $1.4 \text{ cm}^{-1}$  for polyethylene and  $6 \text{ cm}^{-1}$  for TPX. Polyethylene lenses are easily fabricated by pressure moulding of pellets. Allowance must be made for shrinkage of 4% between the moulding temperature ( $325^\circ\text{F}$ ,  $150^\circ\text{C}$ ) and cryogenic temperatures ( $\leq 77 \text{ K}$ ).

## 9. SPECTRAL FILTERS

In the far-IR, wideband, medium-band, and low-pass (long-wavelength transmitting) filters are readily constructed from dielectric materials with suitable absorption properties.<sup>18</sup> The optical characteristics of these materials<sup>18-20</sup> and the techniques for cutting, grinding, and polishing them<sup>21</sup> are well documented.

At submillimeter wavelengths, the choice of suitable dielectric materials is severely limited. At these wavelengths, however, several types of practical filters have been constructed from metal grids. Ulrich<sup>22-24</sup> has given a theoretical description of filters incorporating inductive grids (metal meshes) and capacitive grids (arrays of metal squares supported on dielectric substrates). Low-pass filters with high transmission ( $> 75\%$ ) sharp cut-ons, and good blocking

at short wavelengths have been constructed from series of capacitive grids.<sup>22-28</sup> When these filters are made with dielectric spacers,<sup>30</sup> they accurately follow the theoretically predicted scaling and are mechanically rugged. High-pass filters with very sharp cut-offs ("thick grill filters") have been fashioned of hexagonal close-packed arrays of holes drilled in metal plates<sup>27</sup> where the plate thickness is  $\sim 1.5$  to 2 times the hole diameter,  $d$ . The transmittance is very low below the cut-off frequency,  $\nu_1 = 0.586/d$ , for the lowest propagating mode in a circular waveguide of diameter  $d$ . The transmittance at the peak ( $> 80\%$ ) is somewhat greater than the ratio of hole area to total filter area. The simplest high-pass filters are made of rectangular metal meshes. The transmittance is high (and the reflectivity low) for  $\lambda \lesssim 1.3$  times the grid spacing and drops nearly to zero for  $\lambda \gtrsim 2$  times the grid spacing.<sup>22,29</sup> The cutoff in transmission is not as sharp as that of the thick grill filters. Bandpass filters have been constructed by combining high- and low-pass elements,<sup>24,27</sup> and by using resonant arrays of metal crosses<sup>24,30-34</sup> which serve as hybrids of inductive and capacitive grids.

For submillimeter passbands with  $\Delta\lambda/\lambda \lesssim 0.2$ , the best performance has been achieved with double half-wave (DHW) filters<sup>35,36</sup> (two immediately adjacent Fabry-Perot interferometers combined with low-pass filters to reject all but the fundamental passband). The width of the passband depends on the grid period of the meshes used in the reflecting layers. The mean wavelength depends on the spacing. Convenient fabrication techniques have been devised to produce DHW filters which have accurate, adjustable spacing and which survive mechanical shocks and temperature cycling.<sup>37</sup> Figure 7 shows the transmission curve of a representative DHW filter.<sup>17</sup>



## 10. POLARIMETERS

Measurements of the linear components of polarization of astronomical sources have been made in the far-IR<sup>38-40</sup> and, more recently, at submillimeter wavelengths<sup>41</sup>. The analyzing elements for the far-IR measurements have been rotating grids of parallel conductors made of free-standing wires or of photo-etched ribbons on dielectric substrates. The theory of such grids has been presented by Auton.<sup>42</sup> In a typical design, the actual transmitted intensity through two free-standing wire grids, of wire spacing  $\approx \lambda/5 \approx 3.5 \times$  wire diameter and r.m.s. spacing error  $\approx 5\%$ , is reduced by more than a factor of 100 as the grids are turned from the parallel to the crossed position.

With spectral passbands of the quality shown in Figure 7, it is feasible to incorporate retardation plates into the analysis system and hence to make measurements of all the Stokes parameters of the incoming radiation. Quartz and sapphire are both suitable birefringent materials with well-known optical properties at far-IR/SMM wavelengths and cryogenic temperatures.<sup>19</sup> For each, the difference between the indexes of the E and O rays is nearly independent of wavelength for  $\lambda \gtrsim 60 \mu\text{m}$ . Quartz has the disadvantage that a large difference in the absorption coefficients for the E and O rays causes a significant instrumental polarization. In sapphire, a large difference in the indexes and hence in the reflectivities for the E and O rays again causes a significant instrumental polarization ( $\sim 5\%$ ). This effect can be overcome, however, by using a "sapphire sandwich" composed of a sapphire retardation plate between two thin plates of non-birefringent sapphire<sup>43</sup>.

For measurements of linear polarization, the retardation plate may be replaced by an Abbe/König K-mirror<sup>41,43,44</sup> a device which, unlike a half wave plate, has the property of rotating the image at twice the rate of the mechanical rotation. The K-mirror has the advantage that it is achromatic and hence permits use of a broad passband or changes in the passband. A disadvantage is that

rotation of the image can produce spurious effects if rays entering different portions of the defining aperture are detected with different efficiencies. An achromatic device incorporating two Fresnel rhombs could be used to rotate the plane of polarization without rotating the image.

Since the degree of polarization to be expected at SMM wavelengths from astronomical sources is usually not more than a few percent, measurements must be accurate to a few tenths of a percent or better. One must therefore design a polarimeter in such a way as to suppress the effects of "sky noise" (changes in atmospheric emission and transmission) which limit the statistical accuracy of typical photometric measurements, even for bright sources, to  $\sim 1\%$ . One approach is to rotate the analyzing element at a rate faster than the characteristic frequency of the sky noise under the conditions of the observations<sup>38</sup>. Another approach is to make simultaneous measurements of two components of polarization. To first order, the difference in the signals divided by the sum, e.g.  $S \equiv (V - H)/(V + H)$  where  $V$  and  $H$  are, say, the vertical and horizontal components, is independent of fluctuations affecting both signals equally. This quantity, the "polarization signal",  $S(\theta, \alpha)$ , measured as a function of the angle,  $\theta$ , of the retardation plate at a known position,  $\alpha$ , of the field of view with respect to the instrument should, in principle, give a measure of the source polarization. But since instrumental polarization effects are generally large at submillimeter wavelengths, the source polarization is best derived from the difference  $D(\theta, \alpha_1, \alpha_2) \equiv S(\theta, \alpha_2) - S(\theta, \alpha_1)$  between the values of  $S$  measured at two orientations,  $\alpha_1$  and  $\alpha_2$ .<sup>41,43</sup> To good approximation, the effects of instrumental polarization are removed in taking the difference. With an alt-azimuth telescope, the change in  $\alpha$  is automatically produced by the rotation of the earth. The effects of instrumental polarization can also be removed by comparison of the values of  $S(\theta, \alpha)$  for an unknown source with the values for a

calibration source of known polarization. As yet, very few such calibration sources exist.

An instrument<sup>41,43</sup> designed for submillimeter polarimetry in the Kuiper Airborne Observatory is shown schematically in Figure 8. It has been operated both with a K-mirror, as shown, and with a halfwave retardation plate. An important feature of the instrument, when operated with a retardation plate, is that it minimizes spurious effects due to intensity gradients across the apertures. Such effects can be produced by non-normal reflection near the edge of a lens or by absorption of the electric vector tangent to a conducting surface such as the concentrator surface. The latter effect can become significant in diffraction-limited field optics where the wavelength is non-negligible in comparison with the aperture dimensions. The effect is greatly reduced when (as in this design) the radiation is 100% polarized before reaching the lenses and concentrators.

## 11. ACKNOWLEDGEMENTS

I wish to thank G. Novak and R. Winston for the calculations used in preparing Figure 5 and W. Duncan for calling attention to an error in Fig. 2a of reference 6. I am grateful to my students, former students, and other associates, especially J. A. Davidson, M. Dragovan, D. A. Harper, J. Keene, S. H. Moseley, G. Novak, R. F. Stiening, S. E. Whitcomb, and R. Winston, for their collaboration in work on submillimeter field optics at the University of Chicago. That work and the preparation of this manuscript have been supported primarily by NASA grant NSG-2057.

## 12. REFERENCES

1. F. J. Low, J. Opt. Soc. Amer., 51(11), 1300 (1961).
2. F. J. Low and G. H. Rieke, Methods of Experimental Physics, 12, Part A, 415 (1974).
3. R. Winston J. Opt. Soc. Amer., 60(2), 245 (1970).
4. W. T. Welford and R. Winston, The Optics of Nonimaging Concentrators. Academic Press, New York (1978).
5. D. A. Harper, R. H. Hildebrand, R. Stiening, and R. Winston, Appl Opt., 15 (1), 60 (1976). Notice that the references for this paper appear (misplaced) on 15(1), 144 (1976).
6. R. H. Hildebrand and R. Winston, Appl. Opt., 21(10), 1844 (1982). See errata, Ibid 14(5), 616 (1985).
7. N. S. Nishioka, P. L. Richards, and D. P. Woody, Appl. Opt., 17(10), 1562 (1978).
8. J. Keene, R. H. Hildebrand, S. E. Whitcomb, and R. Winston, R., Appl. Opt., 17(7), 1107 (1978).
9. S. W. Whitcomb, R. H. Hildebrand, and J. Keene, Publ. Astron. Soc. Pac., 92(550), 863 (1980).
10. R. Winston, R. and W. T. Welford, J. Opt. Soc. Amer., 69(4), 532 (1979).
11. A. Rabl, Int. J. Heat Mass Transfer, 20(4), 323 (1977).
12. P. F. Dickson and M. C. Jones, Nat. Bur. Stand. Technical Note 348, (1966).
13. J. C. Mather, Appl. Opt., 21(6), 1125 (1982).
14. D. M<sup>C</sup>Cammon, S. H. Moseley, J. C. Mather, and R. F. Mushotzky, J. Appl. Phys. 56(5), 1263 (1984).
15. A. E. Lange, E. Kreysa, E., S. E. M<sup>C</sup>Bride, P. L. Richards, and E. Haller, Int. J. Infrared and Millim. Waves, 4(5), 689 (1983).

16. J. Clarke, G. I. Hoffer, P. L. Richards, and N. H. Yeh, *J. Appl. Phys.*, 48(12), 4865 (1977).
17. M. Dragovan and S. H. Moseley, *Appl. Opt.* 23(5), (1984).
18. K. R. Armstrong and F. J. Low, *Appl. Opt.*, 12(9), 2007 (1973).
19. E. V. Loewenstein, D. R. Smith, and R. L. Morgan, *Appl. Opt.*, 12(2), 398 (1973).
20. D. R. Smith and E. V. Loewenstein, *E. V.*, *Appl. Opt.*, 14(6), 1335 (1975).
21. C. L. Gupta, and R. C. Tyagi, *Appl. Opt.*, 9(3), 675 (1970).
22. R. Ulrich, *Infrared Physics*, 7(1), 37 (1967).
23. R. Ulrich, *Infrared Physics*, 7(2), 65 (1967).
24. R. Ulrich, *Appl. Opt.*, 7(10), 1987 (1968).
25. G. D. Holah and S. D. Smith, *J. Phys. D: Appl. Phys.*, 5(3), 496 (1972).
26. G. D. Holah and J. P. Anton, *Infrared Physics*, 14(3), 217 (1974).
27. T. Timusk, and P. L. Richards, *Appl. Opt.*, 20(8), 1355 (1981).
28. S. E. Whitcomb, and J. Keene, *Appl. Opt.*, 19(2), 197 (1980).
29. A. Mitsuishi, Y. Otsuka, S. Fujita, and H. Yoshinaga, *Japan. J. Appl. Phys.*, 2(0), 574 (1963).
30. V. P. Tomaselli, C. C. Edewaard, P. Gillan, and K. D. Möller, *Appl. Opt.*, 20(8), 1361 (1981).
31. S. T. Chase, and R. D. Joseph, *Appl. Opt.*, 22(11), 1775 (1983).
32. I. Anderson, *Bell Syst. Tech. J.*, 54(10), 1725 (1975).
33. J. A. Arnaud and F. A. Pelow, *Bell Syst. Tech. J.*, 54(2), 263 (1975).
34. J. E. Davis, *Infrared Physics*, 20(4), 287 (1980).
35. S. D. Smith, *J. Opt. Soc. Amer.*, 48(1), 43 (1958).
36. G. D. Holah, Infrared and Millimeter Waves. Ed., K. J. Button. Vol. 6. (1982).
37. M. Dragovan, *Appl. Opt.*, 23(16), 2798 (1984).

38. W. Cudlip, I. Furniss, K. J. King, and R. E. Jennings, Mon. Not. R. Astr. Soc., 200(3), 1169 (1982).
39. G. E. Gull, R. W. Russell, G. Melnick, and M. Harwit, Astr. J., 85(10), 1379 (1980).
40. G. Dall'Oglio, B. Melchiorri, F. Melchiorri, V. Natale, S. Aiello, and F. Mencaraglia, Planets, Stars, and Nebulae Studied with Photopolarimetry. Ed., T. Gehrels., p. 322, Arizona 1974.
41. R. H. Hildebrand, M. Dragovan, and G. Novak, Astrophys. J. (Lett), 284(2), L51 (1984).
42. J. P. Auton, Appl. Opt., 6(6), 1023 (1967).
43. M. Dragovan and G. Novak, Proc. Symposium on Airborne Astron., NASA/Ames Conf. publication 2353, 335 (1984).
44. H. Naumann, Handbuch der Physik, 29, 217 (1967).

## FIGURE CAPTIONS

Fig. 1. Schematic diagram of a far-IR/SMM field optics system.

Fig. 2. (a) Beam diameter vs. relative aperture,  $R$ , where  $R = \text{aperture radius} \div \text{radius of Airy disk}$ . (The beam diameter is in units of the minimum diameter as  $R \rightarrow 0$ ). (b) Relative throughput vs.  $R$ , normalized to the value for  $R = 1$ .

Fig. 3. Effect of a lens ahead of the focal plane on the angular distribution of rays at the field stop. (a) No lens. (b) Lens inserted. A concentrator accepting the range  $0$  to  $\theta_1$  at every point (shaded regions) will accept some stray rays (e.g. ray  $s$ , which reaches the field stop at  $\theta = 0$ ), and will reject some wanted rays (e.g., ray  $w$ , which reaches the field stop at  $\theta > \theta_1$ ).

Fig. 4. Lens/trumpet concentrator.  $AA'$  is the image of the telescope mirror which would be formed by the lens in the absence of the reflector. With the reflector, the radiation is concentrated to an exit aperture of diameter  $d_2$ .

Fig. 5. Number of reflections vs. acceptance angle,  $\theta_1$ , (and vs. telescope focal ratio). The LTC curve is for a lens/trumpet concentrator in which the small end is truncated by an amount such that the area of the exit aperture is 10% larger than that of the full length LTC.

Fig. 6. Re-imaging field optics. Lenses placed at the focal plane and the pupil stop reimage the primary mirror at a second focal plane containing the field stop.

Fig. 7. Bandpass of a double half wave filter. The central wavelength,  $\lambda_0$ , is easily adjusted by changing spacers between the reflecting grids. The width,  $\Delta\lambda$ , of the passband (FWHM) depends on the periods of the grids. As shown here,  $\lambda_0 = 286 \mu\text{m}$ ,  $\Delta\lambda = 45 \mu\text{m}$ ,  $\Delta\lambda/\lambda = 0.16$ . A capacitive grid is used to block the resonances at  $\lambda_0/2$  and shorter wavelengths.

Fig. 8. Schematic diagram of a submillimeter polarimeter for the Kuiper Airborne Observatory. The incoming radiation passes through a spectral filter, F, and then through an Abbe/König K-mirror, K. The K-mirror is rotated about the optic axis in  $15^\circ$  steps giving  $30^\circ$  steps in the plane of polarization of the transmitted radiation. A fixed parallel wire grid,  $G_1$ , separates the vertical, V, and horizontal, H, components. The light paths are folded (and additional short wavelength filtering is provided) by reflections from the fixed grids  $G_2$  and  $G_3$  which have wires parallel to the planes containing the V and H components respectively. The beams are concentrated using Winston concentrators and detected by  $^3\text{He}$ -cooled bolometers  $B_V$  and  $B_H$ .



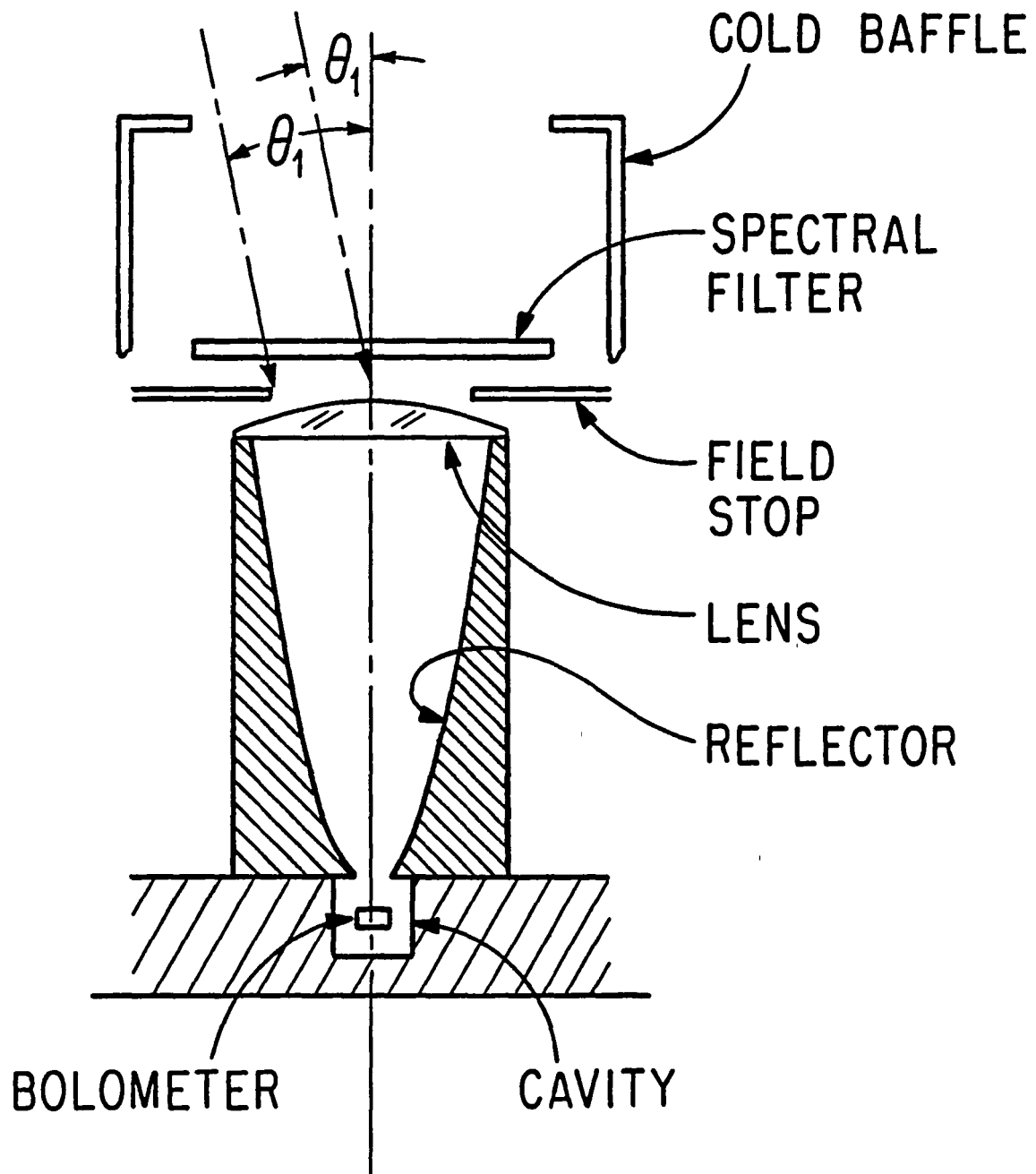


Fig. 1

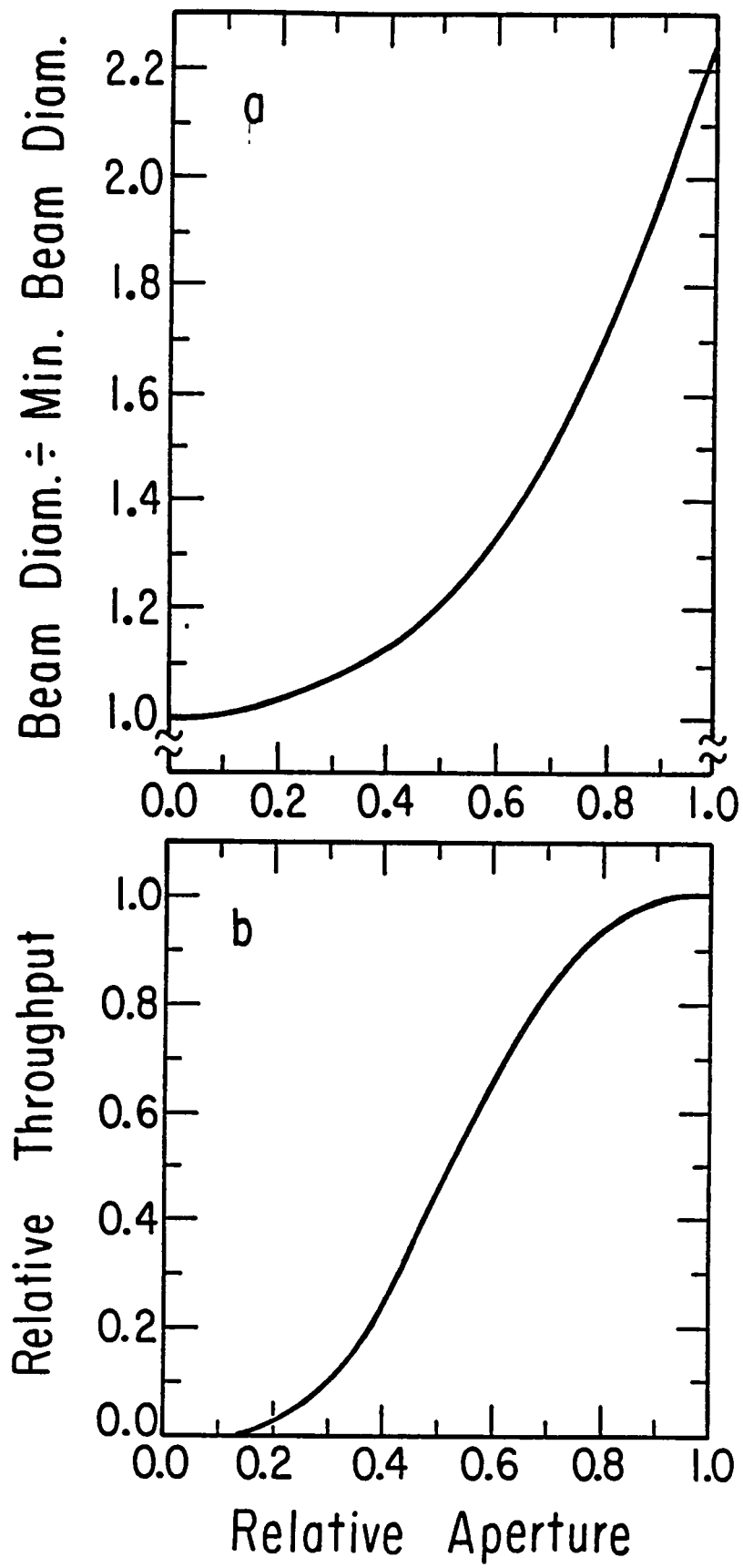


Fig. 2

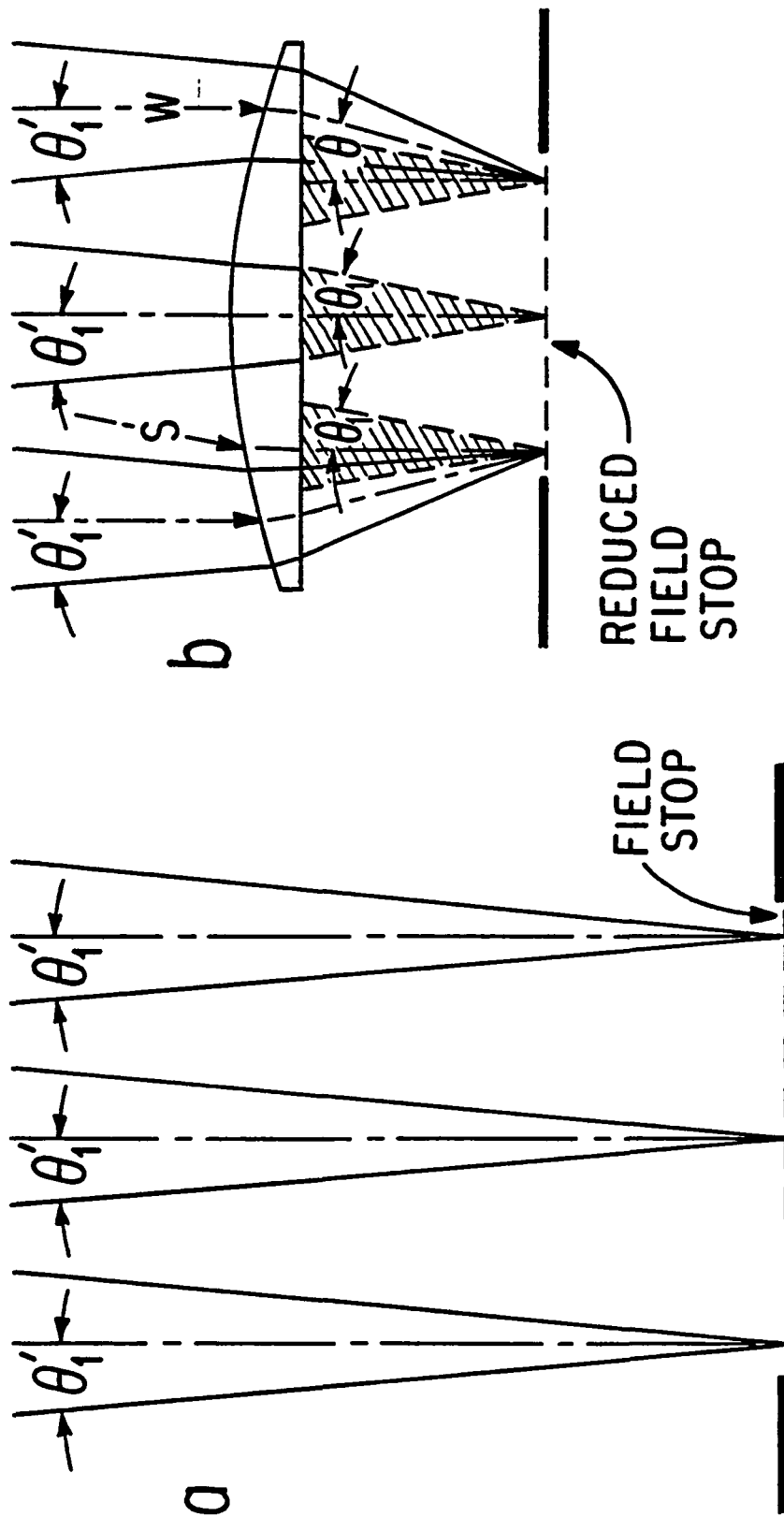


Fig. 3

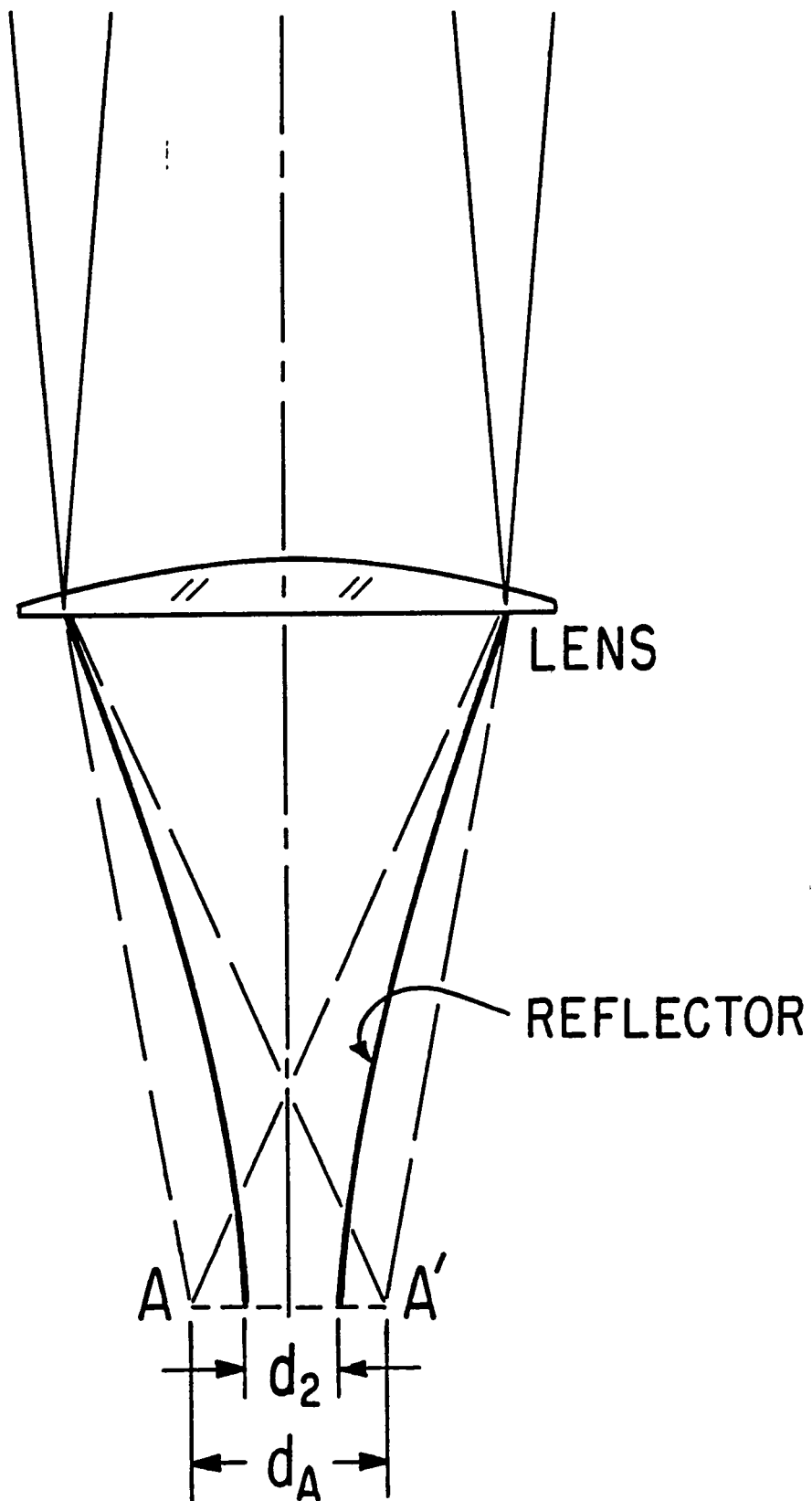


Fig. 4

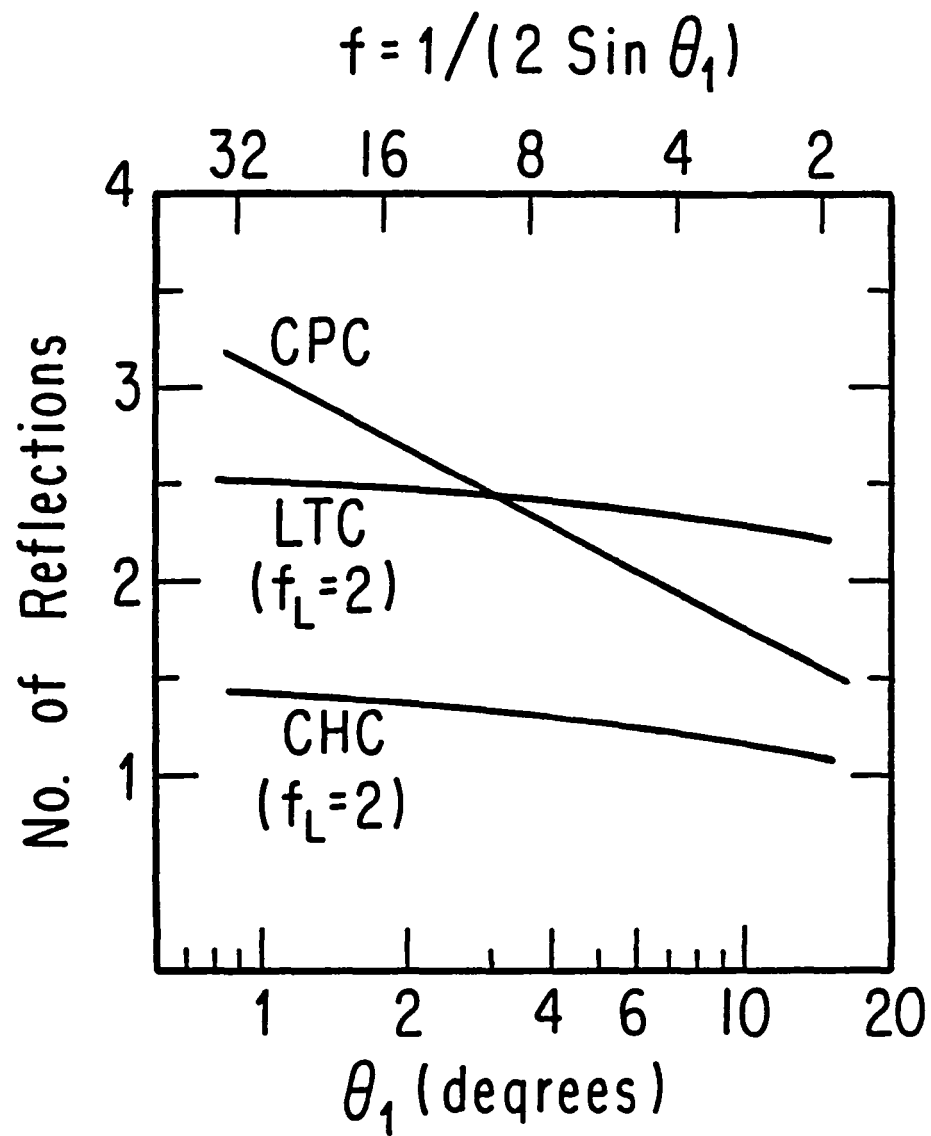


Fig. 5

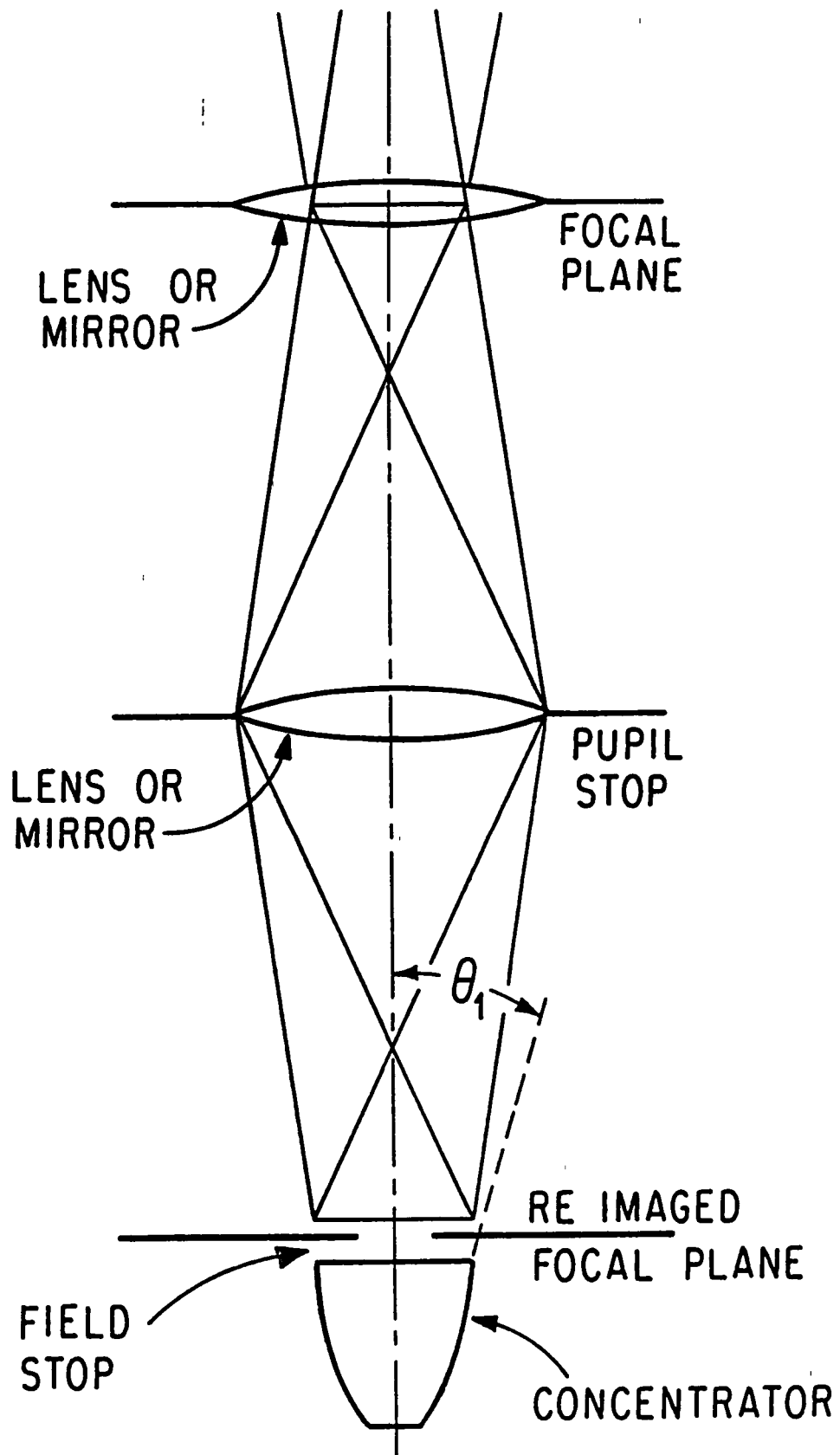


Fig. 6

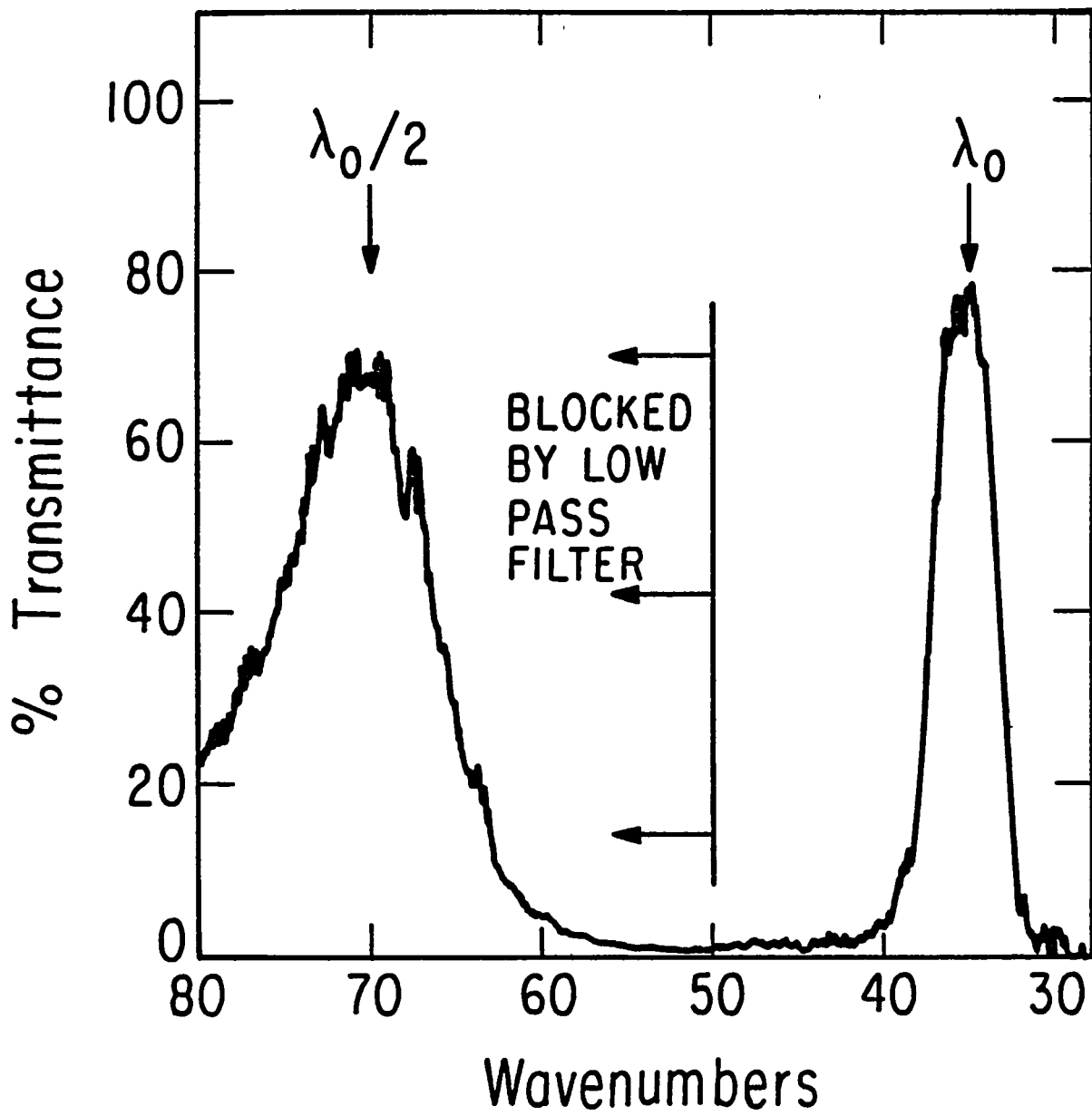


Fig. 7

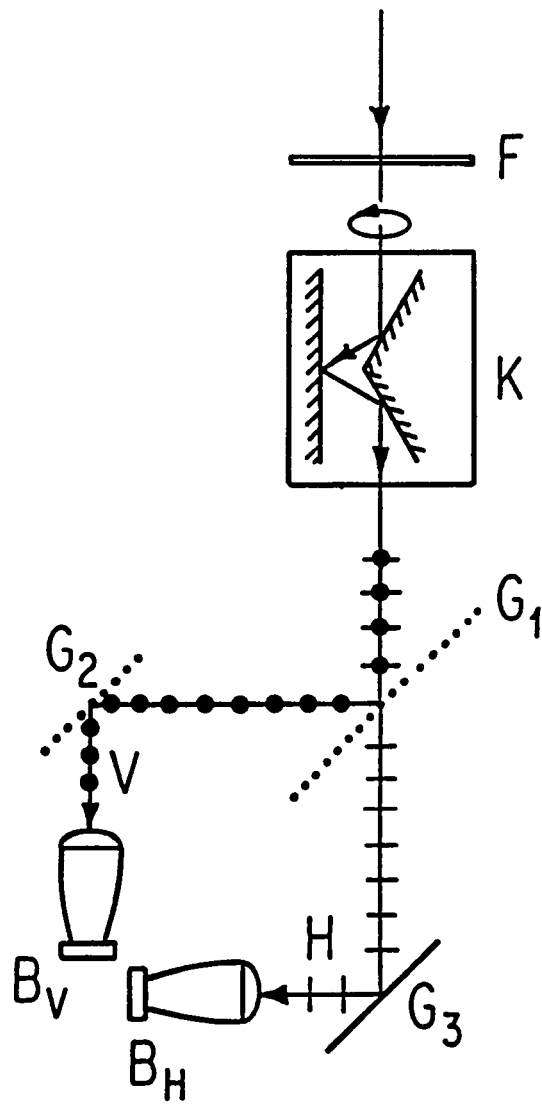


Fig. 8



1 Report No NASA TM-88186		2 Government Accession No		3 Recipient's Catalog No	
4 Title and Subtitle FOCAL PLANE OPTICS IN FAR-INFRARED AND SUBMILLIMETER ASTRONOMY				5 Report Date October 1985	
				6 Performing Organization Code	
7 Author(s) Roger H. Hildebrand				8 Performing Organization Report No 86010	
9 Performing Organization Name and Address Enrico Fermi Institute, University of Chicago, Chicago, IL 60637				10 Work Unit No	
				11 Contract or Grant No	
12 Sponsoring Agency Name and Address National Aeronautics and Space Administration Washington, DC 20546				13 Type of Report and Period Covered Technical Memorandum	
				14 Sponsoring Agency Code 352-02-03	
15 Supplementary Notes Preprint Series #40. Supported by NASA grants. Point of contact: L. C. Haughney, Ames Research Center, MS 211-12, Moffett Field, CA 94035, (415) 694-5339 or FTS 464-5339					
16 Abstract  The construction of airborne observatories, high mountain-top observatories, and space observatories designed especially for infrared and submillimeter astronomy has opened fields of research requiring new optical techniques. A typical far-IR photometric study involves measurement of a continuum spectrum in several passbands between ~30 $\mu\text{m}$ and 1000 $\mu\text{m}$ and diffraction-limited mapping of the source. At these wavelengths, diffraction effects strongly influence the design of the field optics systems which couple the incoming flux to the radiation sensors (cold bolometers). The Airy diffraction disk for a typical telescope at submillimeter wavelengths (~100 $\mu\text{m}$ -1000 $\mu\text{m}$ ) is many millimeters in diameter; the size of the field stop must be comparable. The dilute radiation at the stop is fed through a Winston nonimaging concentrator to a small cavity containing the bolometer.  The purpose of this paper is to review the principles and techniques of infrared field optics systems, including spectral filters, concentrators, cavities, and bolometers (as optical elements), with emphasis on photometric systems for wavelengths longer than 60 $\mu\text{m}$ .					
17 Key Words (Suggested by Author(s)) Nonimaging optics      Submillimeter Field optics              Astronomy Infrared                    Photometry				18 Distribution Statement  Unlimited  Subject category - 89	
19 Security Classif (of this report) Unclassified		20 Security Classif (of this page) Unclassified		21 No of Pages 32	
				22 Price* A03	

**End of Document**